Journal of
Polymer & Composites

https://journals.stmjournals.com/jopc

ISSN: 2321-2810 (Online)
ISSN: 2321-8525 (Print)
Volume 14, Special Issue 3, 2026
DOI (Journal): 10.37591/JoPC

Research JoPC

Influence of Infill Density on Structural Performance of FDM-Processed PET-G Polymer: Experimental Validation through Quadcopter Flight Testing

Sunny Nanade[1],*, Zarvan Movdawalla[2]

Abstract

Polyethylene terephthalate glycol-modified (PET-G) is an amorphous thermoplastic copolymer increasingly adopted in structural applications through fused deposition modeling (FDM). However, the correlation between FDM processing parameters, especially infill density, and mechanical performance of PET-G parts remains inadequately characterized under real-life loading conditions. This study investigates how infill density (10% and 30%, grid pattern) influences the structural integrity of FDM-processed PET-G components, validated experimentally through quadcopter airframe fabrication and flight testing. Two geometrically identical X-configuration frames (450 mm motor-to-motor diagonal) were fabricated with identical processing parameters (layer height 0.25 mm, nozzle temperature 240 °C, bed temperature 75 °C, three perimeters, four top/bottom solid layers) differing only in infill density. Both frames were assembled with M3 fasteners and subjected to outdoor flight tests including hover, translation, and repeated takeoff-landing cycles. The 10% infill frame (600 g) suffered catastrophic brittle fracture at the arm-body interface within five flights, initiating at bolt hole stress concentrations and propagating through the sparse internal polymer lattice. The 30% infill frame (690 g) completed over 20 flights without structural degradation. The threefold increase in polymer volume fraction provided significantly higher energy absorption and load distribution despite only a 15% mass increase and 5–8% reduction in flight endurance. These results demonstrate that infill density fundamentally controls effective mechanical properties of FDM-processed PET-G, and that bulk material datasheet values cannot be directly applied to printed structures.

Keywords: PET-G polymer, fused deposition modeling, polymer processing, infill density, thermoplastic mechanical properties, additive manufacturing, structural polymer applications, UAV frames

***Author for Correspondence**
Sunny Nanade

[1]Assistant Professor, Department of Mechatronics Engineering, Mukesh Patel School of Technology Management & Engineering, SVKM's NMIMS, Mumbai, Maharashtra, India
[2]Student, Department of Mechanical Engineering, Mukesh Patel School of Technology Management & Engineering, SVKM's NMIMS, Mumbai, Maharashtra, India

Received Date: March 20, 2026
Accepted Date: March 31, 2026
Published Date: May 12, 2026

Citation: Sunny Nanade, Zarvan Movdawalla. Influence of Infill Density on Structural Performance of FDM-Processed PET-G Polymer: Experimental Validation through Quadcopter Flight Testing. Journal of Polymer & Composites. 2026; 14(Special Issue 3): S644–S656p.

INTRODUCTION

Fused deposition modeling (FDM) is an additive manufacturing process that uses extrusion of the polymer melt, i.e. thermoplastic filament, to deposit a layer of a 3D product by heating filament material and then extruding it through a thin precision nozzle to build the layer-by-layer structure of the part [1, 2]. Being a polymer processing method, FDM forms parts whose mechanical behavior is dictated not only by the base polymer chemistry, but also by processing variables such as nozzle temperature, layer height, deposition speed, and most importantly, infill density - internal fill fraction of the part envelope that dictates the effective polymer volume of the part [2, 3].

Polyethylene terephthalate glycol-modified (PET-G) is among the thermoplastics traditionally handled through FDM, and the material has attracted a lot of attention as a structural material. PET-G is an amorphous thermoplastic copolymer created by introducing cyclohexane dimethanol (CHDM) into PET backbone, which disturbs the chain regularity, crystallization under strain and results in a completely amorphous polymer that has high ductility than semi-crystalline PET [4]. PET-G has a glass transition temperature (Tg) of 80–85 °C, bulk tensile strength of 50–53 MPa, and elongation at break of 18–23%, which means it can be used in impact-loaded structural applications [4, 12].

PET-G has emerged as a preferred material for structural applications in FDM due to several distinct advantages over alternative thermoplastics. Unlike PLA, which suffers from brittle failure and low heat deflection temperature, PET-G offers a balanced combination of strength, ductility, and thermal stability suitable for load-bearing components [14, 16]. The amorphous nature of PET-G results in minimal warping during printing, enabling the fabrication of large structural parts without the need for a heated enclosure, which is a significant practical advantage for drone frame manufacturing [15]. Additionally, PET-G demonstrates superior chemical resistance and weatherability compared to ABS, making it suitable for outdoor structural applications where exposure to moisture and varying temperatures is expected [14, 17].

There is however a fundamental disconnect between the bulk polymer material characteristics that are displayed on the datasheets and the actual mechanical behavior of FDM-processed parts. Density infillament level is a direct way to control the internal polymer volume fraction forming a cellular or lattice-like mesostructure, the effective stiffness and strength of which are significantly less than those of solid material [5, 7]. Although a number of studies have defined infill density effects by conducting laboratory coupon testing [5, 6], there is not much information about the effect of these parameters on structural performance under actual operational loading conditions where complex, dynamic, multi-directional loading occurs.

This gap is filled by the study by producing two geometrically equal PET-G polymer geometrically identical frames using FDM and various infill densities (10% and 30%), and testing them as unmanned aerial vehicle (UAV) airframes under operational flight conditions. Due to the influence of vibration, aerodynamic forces and high-energy impact events during landing, UAV frames are suitable as a platform to test a validation [8, 9]. The experimental method is used to make direct comparison of structural performance in conditions that cannot be reproduced by the normal tensile or flexural coupon testing. The frames were designed in respect of the SAE AeroThon 2026 competition.

PET-G Polymer Properties and FDM Processing

PET-G is polyester based thermoplastic. The glycol modification substitutes part of the ethylene glycol monomer by CHDM, which forms big rings of cyclohexane that cannot be packed and crystallized into chains. This amorphous form has a number of benefits to FDM processing [4]:

- Minimal warping (no heated chamber) due to low shrinkage of cooling.
- Large processing temperature range (230–250 °C nozzle temperature)
- Strong interlayer adhesion because of amorphous chains motility over Tg.
- Chemical resistance better than PLA.
- Moderate strength of impact that is used in structural work.

The mechanical properties of PET-G processed through FDM are significantly influenced by printing parameters including nozzle temperature, layer height, infill density, and raster orientation [15, 16]. Bulk PET-G exhibits tensile strength in the range of 50–53 MPa, Young's modulus of 2.0–2.1 GPa, and elongation at break of 18–23%. However, FDM-processed PET-G components typically demonstrate reduced effective properties relative to bulk material, with tensile strength ranging from 28–45 MPa depending on infill density and print orientation [14, 18]. The glass transition temperature of 80–85 °C provides dimensional stability under moderate thermal loading, while the amorphous structure ensures consistent mechanical properties regardless of processing-induced crystallinity variations. Recent studies on the optimization of FDM process parameters have demonstrated that nozzle temperature and infill strategy are critical factors determining the final mechanical performance of PET-G printed parts [15, 16].

Table 1 compares key polymer properties of common FDM thermoplastics relevant to structural applications.

- *Polylactic acid (PLA):* A bio-derived semi-crystalline polyester, with good printability, which has brittle failure properties (3–6% elongation at break), and cannot be used in impact-loaded applications [3, 6].
- *Acrylonitrile butadiene styrene (ABS):* An amorphous terpolymer that offers better toughness through rubber phase modulation, yet needs heated chamber in order not to warp when used in large format printing [3].
- *Nylon (polyamide):* This is a semi-crystalline polymer that has excellent mechanical characteristics but has high moisture absorption and thus performance is adversely affected in a humid environment.
- *PET-G:* Chosen in this study due to it having a combination of properties: sufficient tensile, moderate Tg, low warping (possible to open-frame print), and reasonable cost (costs around $32/kg in the local market) [4].

Infill density plays a critical role in determining the energy absorption capacity and impact resistance of FDM-processed PET-G structures [14, 16]. At lower infill densities, the cellular mesostructure created by the infill pattern enables progressive crushing and energy absorption through controlled deformation of the internal lattice, functioning analogously to engineered foam structures. Studies have demonstrated that moderate infill densities (20–40%) can provide optimal energy absorption efficiency, where the ratio of absorbed energy to component weight is maximized [17, 18]. Higher infill densities increase peak load capacity but reduce specific energy absorption due to the additional material weight. The infill pattern geometry also significantly influences impact behavior, with triangular and gyroid patterns exhibiting superior energy absorption compared to rectilinear patterns due to their multi-directional load distribution characteristics [14, 15]. Understanding these relationships is critical for designing FDM polymer frames that must withstand dynamic impact events during operation.

Research Objectives

This study aims to:

1. Describe how infill density influences structural performance of PET-G polymer material processed by FDM, and operated under loading condition.
2. Measured the trade off between the volume fraction (infill density) of polymer and structural integrity.
3. Under-reinforced FDM polymer structures Leakages in documents and fracture nature.
4. Offer useful instructions on the choice of infill density in load bearing PET-G polymer parts

Table 1. Comparison of polymer properties for common FDM thermoplastics.

Property	PLA	ABS	PET-G	ASA
Tensile Strength (MPa)	50–65	35–45	50–53	40–50
Tg (°C)	55–65	100–105	80–85	100
Elongation at Break (%)	3–6	10–20	18–23	15–25
Warping Tendency	Low	High	Low	High
UV Resistance	Poor	Poor	Moderate	Excellent
Heated Chamber Required	No	Yes	No	Yes
Cost ($/kg, approx.)	20–25	22–28	25–32	30–35

MATERIALS AND METHODS

Frame Design

The frame is designed on the SolidWorks CAD software and adhered to the X-configuration architecture of a quadcopter. Amongst the design specification were:

- *Spacing of motors to motors:* 450 mm.
- *Modular print:* individual arms and plate in the middle of the body were printed separately.
- M3 fasteners Bolt-based assembly.
- *Printing material:* thermoplastic filament of PET-G.
- *Critical tolerance:* ±.25 mm to mount features.
- *General tolerance:* 0.5 mm of non critical features (±)

The modular construction was required by the size of printer build volumes (Aion Mk3 by Dividebyzero) and also provided other advantages such as easy replacement of damaged parts and less usage of material.

Figure 1 shows the entire CAD assembly of the modular X-configuration of the arm parts and the center mounting plate, while Figure 2 presents the frame dimensional specifications including top and isometric views with critical dimensions.

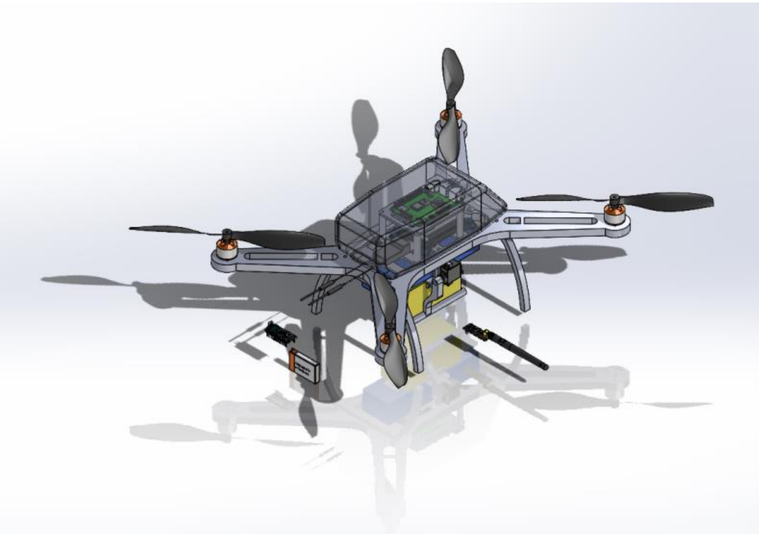

Figure 1. CAD model of modular quadcopter frame. X-configuration with 450mm motor-to-motor spacing. Modular design enables individual component replacement.

Table 2. FDM manufacturing parameters for frame fabrication.

Parameter	Frame 1 (blue)	Frame 2 (grey)
Layer Height	0.25 mm	0.25 mm
Nozzle Temperature	240°C	240°C
Bed Temperature	75°C	75°C
Print Speed	50 mm/s	50 mm/s
Infill Pattern	Grid	Grid
Infill Density	10%	30%
Wall Lines (Perimeters)	3	3
Top/Bottom Layers	4	4
Cooling Fan	40%	40%
Total Weight	600 g	690 g
Print Duration	20 hours	26 hours
Material Cost	$18	$21

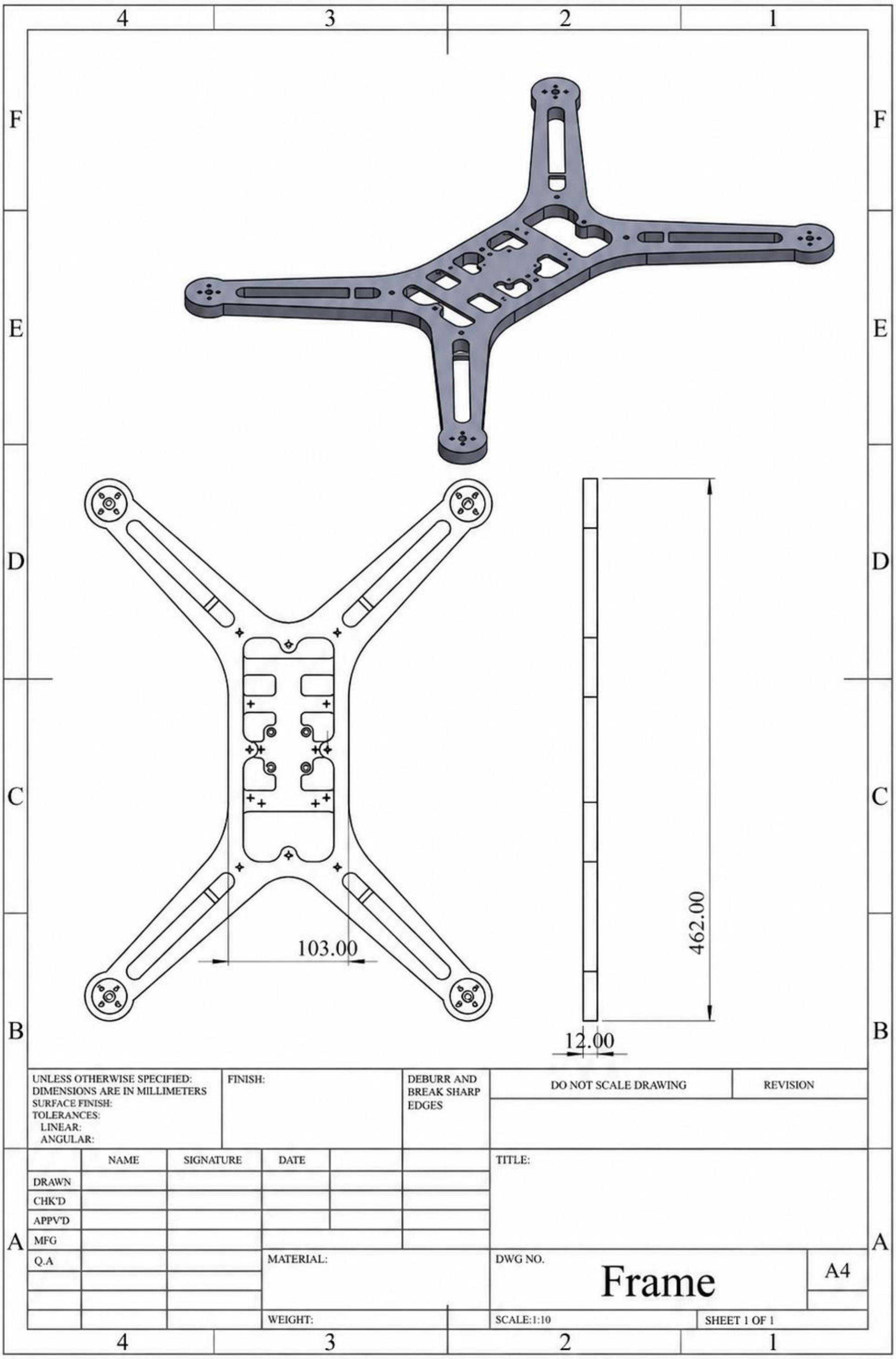

Figure 2. Frame dimensional specifications showing top and isometric views with critical dimensions.

Manufacturing Parameters

All frame components were manufactured using FDM technology on an Aion Mk3 3D printer. Table 2 summarizes the manufacturing parameters for both frame iterations.

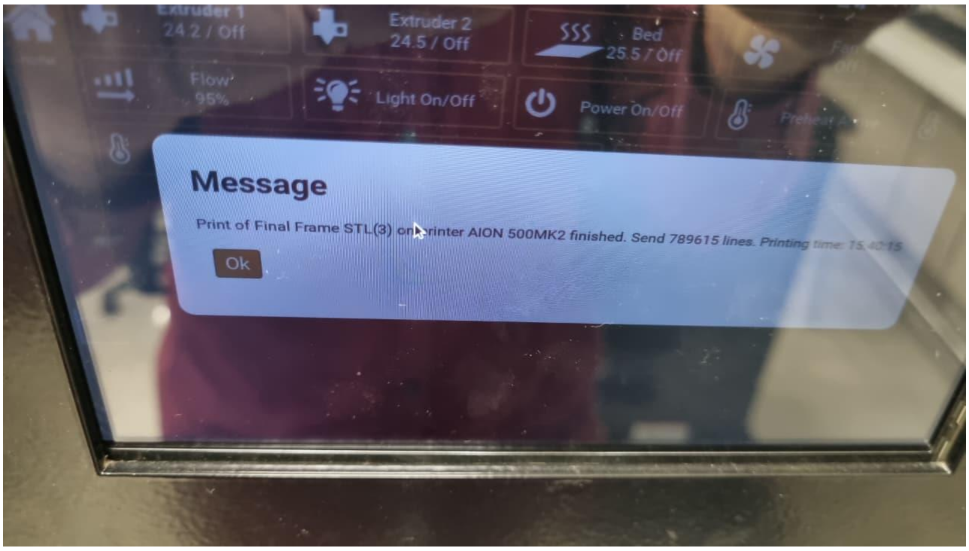

Figure 3. Print completion notification showing 24-hour fabrication duration for major frame components.

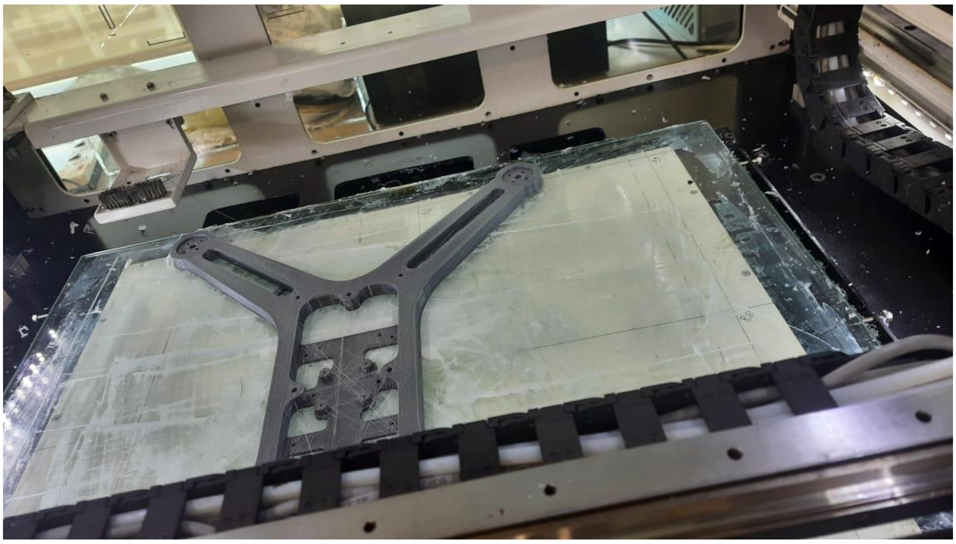

Figure 4. Frame 2 (30% infill) immediately following print completion, showing surface finish and dimensional accuracy.

The manufacturing strategy maintained constant parameters except infill density, enabling isolation of this variable's effect on structural performance. Grid infill pattern was selected for its balance between strength and print time. Figure 3 illustrates the print completion timeline for the major frame components, and Figure 4 shows Frame 2 immediately following print completion, confirming the surface finish and dimensional accuracy achieved.

Assembly and Integration

Following fabrication, frame components were assembled using M3 stainless steel bolts with nylon-insert lock nuts. The complete quadcopter system integrated:

- *Motors:* 4x brushless DC motors (specification withheld)
- Electronic Speed Controllers (ESCs)
- Flight controller with GPS and IMU
- *Battery:* LiPo 3S/4S configuration
- *Propellers:* 10-inch diameter

ISSN: 2321-2810 (Online), ISSN: 2321-8525 (Print)

Testing Protocol

Both frames underwent flight testing in outdoor conditions. Testing included:

- Hover stability assessment
- Controlled takeoff and landing maneuvers
- Forward/lateral translation
- Altitude hold performance
- Emergency landing procedures

Flight duration and impact events were documented for structural performance evaluation. No formal drop testing or destructive testing was performed prior to operational use.

RESULTS

Frame 1 Performance (10% Infill)

Frame 1 that was fabricated using 10 percent grid infill density showed good performance characteristics initially. The frame was complete and illustrated:

- *Mass:* 600 grams
- Smooth surface (acceptable) and surface dimension (acceptable)
- Effective assembling of electronic components.
- Ground level hover attributes on the first flights.

The initial four flight operations did not go against plan. In the course of the fifth flight, which was approached in moderate wind conditions (approximately 3–5 m/s), the plane landed with a firm landing and the impact velocity was estimated 1–2 m/s. The effect of this was disastrous structural failure at the arm-to-body mounting interface. Table 3 summarizes the complete operational performance data for Frame 1.

Upon analysis of the failure:

- Brittle fracture with clean through arm mounting point.
- Plastic deformation is little.
- Failure was triggered at stress concentration in and around bolt holes.
- Internal infill structure had poor distribution of loads.
- About 6 percent of cross-sectional area was load-bearing infill material.

Figure 5 shows the failure location and fracture surface characteristics.

Frame 2 Performance (30% Infill)

Following failure analysis of Frame 1, Frame 2 was fabricated with identical geometry but 30% infill density, tripling the internal polymer volume fraction. This modification resulted in:

- *Mass:* 690 grams (15% increase)
- *Print duration:* 26 hours (30% increase)
- *Material cost:* $21 (17% increase)

Table 3. Frame 1 operational performance summary.

Parameter	Value
Total mass	600 g
Successful flights	5
Cumulative flight time	27 minutes
Failure mode	Brittle fracture at arm joint
Impact velocity (estimated)	1-2 m/s
Material cost	$18
Print duration	20 hours

Figure 5. Frame 1 structural failure at arm mounting joint. Clean brittle fracture indicates insufficient internal reinforcement from 10% infill density.

Frame 2 has successfully completed over 20 flight operations as of this report, including several landing impacts estimated to exceed the force that caused Frame 1 failure. No structural degradation or crack initiation has been observed. Figure 6 presents a flight test sequence collage showing Frame 2 during operational testing. Table 4 provides a detailed comparison of Frame 1 and Frame 2 performance metrics.

Flight performance comparison:

- *Hover time per battery:* Reduced approximately 2–3 minutes (5–8% decrease)
- *Control responsiveness:* No measurable difference
- *Vibration characteristics:* Comparable to Frame 1
- *Structural integrity:* No failures observed

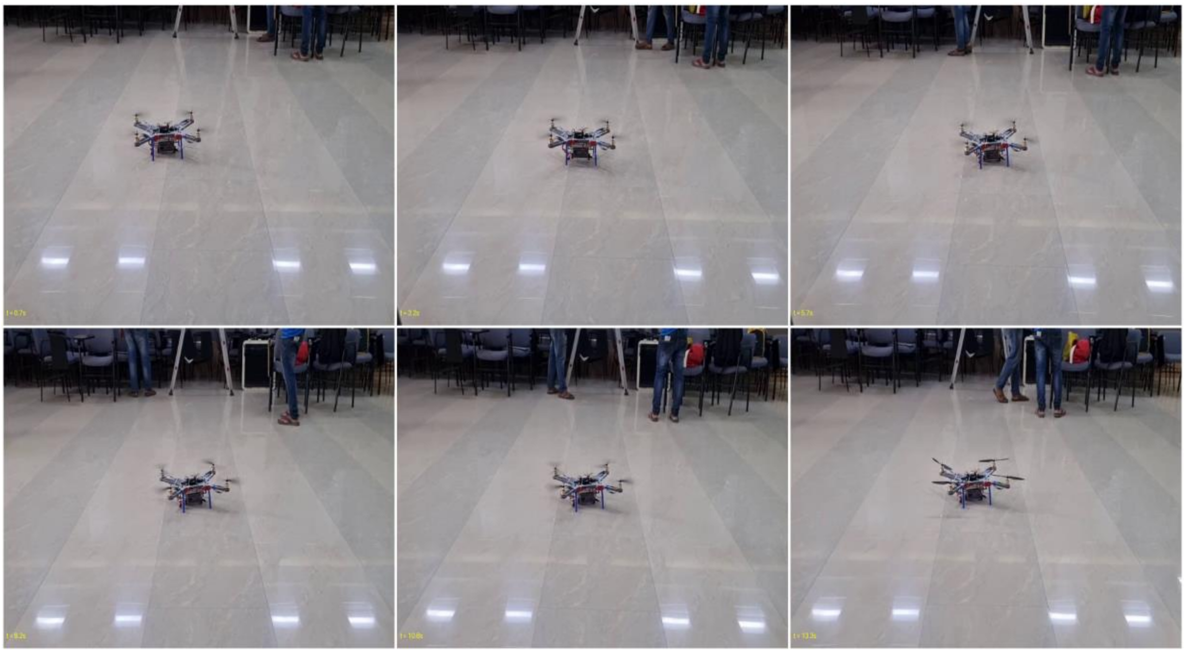

Figure 6. Flight test sequence of Frame 2 (30% infill PET-G). Sequential frames extracted from flight video demonstrate stable hover and controlled maneuvers. No structural degradation observed through 20+ flight cycles.

Table 4: Comparative performance: Frame 1 vs Frame 2.

Parameter	**Frame 1 (10%)**	**Frame 2 (30%)**
Mass	600 g	690 g
Infill Density	10%	30%
Successful Flights	5	20+
Cumulative Flight Time	27 min	190+ min
Structural Failures	1 (catastrophic)	0
Print Duration	20 hours	26 hours
Material Cost	$18	$21
Flight Time per Battery	15 min	12-13 min

Failure Analysis

The mechanism of failure evident in the Frame 1 may be explained by the lack of inner polymer volume to spread the impact loads. The 10% grid fill develops a polymer lattice which is sparse with few load paths between the outer perimeter walls. During impact loading, the stress concentrations at the mounting interface were greater than the local effective yield strength of the low-density polymer mesostructure and therefore the rate of crack propagation was high through the infill region [5].

Frame 2 has an infill of 30 percent which offers about 3 times higher polymer density, an interior which forms a stronger load distribution system. The elevated volume of polymer in the infill area enables impact energy dissipation of the structure via the large structural volume that is in agreement with the correlation among relative density and energy absorption capacity in cellular polymer structures [7].

It is important to notice that there was no interlayer delamination in both frames. All fractures were made in through the bulk polymer material, indicating that sufficient inter-layer chain interdiffusion was made in the processing temperature of 240 °C. This proves that interlayer bonding strength was not the limiting factor with the structural failure during load under operations [2, 3].

DISCUSSION

Polymer Volume Fraction and Effective Mechanical Properties

It provides evidence that the internal polymer volume fraction, determined directly by infill density, is the most influential determinant of structural performance of PET-G components processed using FDM. Whereas bulk PET-G has tensile strength of 50–53 MPa, FDM parts with lower infill do form a cellular mesostructure whose effective properties are proportional to relative density, just like cellular solid mechanics theory predicts [5, 7].

The internal lattice at 10 percent grid fill takes up nearly 6 percent of the area cross section in the failure point (including the perimeter walls and the solid layers at the top and bottom). This thin polymer meshwork was not strong enough to dissipate impact energy causing disastrous brittle fracture forming at stress concentrations along the bolt holes. When internal polymer volume is increased threefold at 30% infill, it forms an equivalent of a denser load-distribution network that has much more material to absorb energy at impact [5, 6, 13].

According to the failure behavior observed, we deduce the levels of effective strengths:

- 10% infill: 20–30% of bulk PET-G strength (10–16 MPa effective)
- 30% infill: 50–60% of bulk PET-G strength (25–32 MPa effective)

These estimates are in agreement with published data on infill density-mechanical property relationships in FDM thermoplastics [5, 6], but to be quantitatively validated formal coupon testing is needed.

Fracture Mechanics and Polymer Failure Behavior

The clean break fracture through the arm mounting point with a slight plastic deformation observed is an indicator of the behavior of the PET-G polymer under impact loads at lower levels of infill densities. Although PET-G is ductile in nature (18–23% elongation at break in bulk shape), the 10% infill mesostructure imposes conditions of brittle like failure [11]:

- Stress concentrations at bolt holes (stress concentration factor ≈ 2–3) exceed local yield strength
- Sparse infill lattice provides insufficient constraint for plastic zone development
- Crack propagation follows the path of minimum resistance through the low-density internal structure
- Limited energy absorption prior to catastrophic failure

The fact that no interlayer delamination was found in either frame can be attributed to the fact that the processing parameters (240 °C nozzle temperature, 0.25 mm layer height) provided sufficient interdiffusion of the polymer chains across layer interfaces. This confirms the fact that failure was not predetermined by the lack of interlayer bonding; instead, the small polymer volume fraction in the infill area dictated failure [2, 10].

Conclusions to Polymer Processing through FDM

The findings can be used by FDM as a polymer processing process in a number of ways:

- *Property Relationship:* Process The infill density should be considered as a significant processing parameter that effectively changes the material properties. Datasheet information of standard polymers is relevant only to solid (100% infill) components. The reduced infill forms a cellular mesostructure that designers need to consider in estimating component strength [2, 7].
- *Safety Factors:* FDM polymer components should have higher safety factors than injection-molded or extruded components with exception being impact-loaded applications in which the cellular infill structure constrains energy absorption [6].

- *Weight Strength Optimization:* The 15 percent mass increment by tripling infill density (10 percent to 30 percent) brought a disproportionate enhancement in structural reliability (15 flights to 20 or more flights). The higher-density polymer design has a lower price/flight minute cost, which implies that non-linear property scaling with infill density [5, 7].
- *Prototype Test:* FDM polymer components that are to be used in structural service are to be tested during fictitious loading. Laboratory coupon data gives requisite yet inadequate foundations to design because actual loading is associated with complicated multi-axial loads and impact occurrences that are not encompassed by standard tensile testing [12].

Comparison with Published Literature

The trend of increment in structural performance with the increase in infill density is similar to Fernandez-Vicente et al. [5], who found the tensile strength incremental rates of about 30 to 80 of the solid material values with the increment in the infill density of the ABS polymer. According to Popescu et al. [2], a review of numerous studies performed confirmed the assertion that infill density is one of the most significant FDM processing parameters in all the prevalent thermoplastics. In their systematic review, Dey and Yodo [7] also found infill density to be the main determining factor of mechanical performance.

The brittle failure mode of 10% infill density agrees with Rodriguez-Panes et al. [6], who reported that low content of infill density PLA and ABS specimen showed lower ductility than higher content of infill density specimen. These laboratory results are relevant to PET-G polymer in operational impact loading conditions, which assures us that our results can be generalized to polymer types and loading regimes.

In a previous experiment carried out by the authors [13] gesture-driven robot chassis was tested using 3D-printed polymer frames with the purpose of proving the suitability of FDM-processed polymers to structural uses, although pointing out the significance of material choice and optimization of processing parameters.

Limitations

This research has a number of limitations which must be mentioned:

- *Sample size:* Only two frames were made and experimented. Statistical deviation of material properties, printing conditions and loading situations were not described.
- *Controlled testing:* There was no mechanical testing (tensile, flexural, impact) done. All the performance data is based on operational use.
- *Environmental control:* Frames were printed on different days possibly under different conditions (ambient temperature, moisture content of the filament, leveling of the bed). These were not measured or controlled variables.
- *Quantification of the load:* The impact forces of landing were not measured but were estimated. Real conditions of loading are not known.
- *Long term durance:* Frame 2 has not had many months of active working time. There were no long-term effects such as UV degradation, thermal cycling and fatigue.
- *Thermal analysis:* Thermal values of the motor and heating of the frame were not recorded. The glass transition temperature of PET-G (80–85° C) might be surpassed in the vicinity of motors, but no thermal deformation was observed.

Future Work

There are some avenues of research that may follow up this work:

1. PET-G polymer coupons at infill densities (10%-100%) were systematically subjected to mechanical test to determine effective material properties and establish process-property linkages [2, 7].

2. Predictive structural design of FDM polymer components with infill density-dependent material model, using finite element analysis.
3. Alternative infill pattern (honeycomb, triangular, gyroid) and the impact of infill pattern on PET-G polymer mechanical anisotropy [5, 6] are investigated.
4. Options of variable infill density optimization with increased polymer volume fraction concentrated at the stress-critical regions.
5. PET-G polymer durability testing- Long-term environmental degradation of PET-G polymer under the UV exposure and thermal cycling condition [11, 12].
6. Comparison using other FDM thermoplastics (ASA, Nylon, carbon fiber reinforced polymers) under the same test conditions.

CONCLUSIONS

This relative examination of FDM-processed PET-G polymer frames reveals that the degree of infill density, as a polymer processing factor, decisively controls the performance of the thermoplastic components generated through printing. Key findings include:

1. PET-G frame polymer with infill density 10 percent broke down dramatically following 5 flights and 27 minutes of operation time, which showed brittle fracture process of the internal polymer structure, which is a sparse polymer network.
2. Frames of 30 percent infill density (three times higher volume fraction of internal polymer) flew 20 or more and 190 or more minutes with no structural degradation.
3. The 15% mass increment (600 g to 690g) due to higher polymer volume fraction decreased only by 5 to 8% flight endurance.
4. Brittle fracture that occurred due to the lack of polymer volume to redistribute loads and not interlayer delamination proved failure mode, which established sufficient interdiffusion of polymer chains during FDM processing at 240 °C.
5. Direct application of bulk material characteristics of PET-G polymer to FDM components is not possible without considering the cellular microstructure that is formed by choice of infill density.

In the case of structural polymer components produced through FDM, the following is recommended in this study:

- Impact-loaded applications of PET-G polymer require minimum 30% infill density.
- Consideration of infill density as a significant polymer processing factor impacting on effective mechanical properties.
- Modular design style of design to allow replacement of components at component level in case of iterative development.
- FDM polymer structures have been tested under realistic loading conditions have to be empirically validated because laboratory coupon data is not enough to design structures.

FDM fabrication using PET-G material is feasible in building structural uses in student contests and quick prototyping. The balanced characteristics of the polymer, such as sufficient strength, low warpage, good interlayer bonding and moderate price (20–25 per frame) make it applicable in applications where impact resistance is needed but the cost and complexity of carbon fiber composites are prohibitive. The parameter optimization of manufacturing (especially infill density selection) cannot be considered as secondary variable of the structural design process.

Future research ought to aim at the quantitative polymer characterization over infill parameter spaces and formulate process-property models that will allow predictive design of FDM polymer structures.

REFERENCES

1. Ngo TD, Kashani A, Imbalzano G, Nguyen KTQ, Hui D. Additive manufacturing (3D printing): A review of materials, methods, applications and challenges. Compos Part B Eng. 2018;143:172–196.

2. Popescu D, Zapciu A, Amza C, Baciu F, Marinescu R. FDM process parameters influence over the mechanical properties of polymer specimens: A review. Polym Test. 2018;69:157–166.
3. Gebrehiwot SZ, Espinosa-Leal L, Linderbäck C, et al. The effect of 3D printing process parameters on the mechanical properties of PLA and ABS materials. IOP Conf Ser Mater Sci Eng. 2019;659:012080.
4. Srinivasan R, Ruban W, Deepanraj A, Bhuvanesh R, Bhuvanesh T. Effect on infill density on mechanical properties of PETG part fabricated by fused deposition modelling. Mater Today Proc. 2020;27:1838–1842.
5. Fernandez-Vicente M, Calle W, Ferrandiz S, Conejero A. Effect of infill parameters on tensile mechanical behavior in desktop 3D printing. 3D Print Addit Manuf. 2016;3(3):183–192.
6. Rodríguez-Panes A, Claver J, Camacho AM. The influence of manufacturing parameters on the mechanical behaviour of PLA and ABS pieces manufactured by FDM: A comparative analysis. Materials. 2018;11(8):1333.
7. Dey A, Yodo N. A systematic survey of FDM process parameter optimization and their influence on part characteristics. J Manuf Mater Process. 2019;3(3):64.
8. Azarov AV, Antonov FK, Golubev MV, Khaziev AR, Ushanov SA. Composite 3D printing for the small size unmanned aerial vehicle structure. Compos Part B Eng. 2019;169:157–163.
9. Mohd SA, Yusoff Y, Majid MSA, et al. Additive manufacturing for aerospace application. IOP Conf Ser Mater Sci Eng. 2021;1051:012005.
10. Czyżewski P, Bieliński M, Sykutera D, et al. Influence of extruder's nozzle diameter on the improvement of functional properties of 3D-printed PLA products. Polymers. 2022;14(2):356.
11. Lužanin O, Movrin D, Plancak M. Impact of processing parameters on tensile strength, in-process crystallinity and mesostructure in FDM-fabricated PLA specimens. Rapid Prototyp J. 2019;25(8):1398–1410.
12. Tanikella NG, Wittbrodt B, Pearce JM. Tensile strength of commercial polymer materials for fused filament fabrication 3D printing. Addit Manuf. 2017;15:40–47.
13. Nanade S, Gharat E, Lakhe A, Shah R. Evaluating chassis designs for gesture-driven robots: A study of iron, acrylic, and 3D printed solutions. J Polym Compos. 2025;13(S5):S686–S692.
14. Kirubakaran G, Kannan CS, Anbalagan RR, Palanisamy S, Alfarraj SA, Alharbi SA, Abbas M, Kalathil S, Belay M. Taguchi-based experimental optimization coupled with explainable machine learning for predictive modelling of FFF-printed CF-PA composites. Int J Adv Manuf Technol. 2026. https://doi.org/10.1007/s00170-026-17709-2.
15. Fitriyana DF, Rudianzah TS, Palanisamy S, Firmansyah HN, Darsono FB, Ismail R, Siregar JP, Cionita T, Alfarraj SA, Alharbi SA, Abbas M, Kalathil S, Belay M. Investigation of the effect of nozzle temperature on the properties of 3D printed PET filament from plastic bottle waste. Int J Adv Manuf Technol. 2026;142:4073–4085.
16. Fitriyana DF, Palanisamy S, Wicaksana YS, Anis S, Rasgianti, Ismail R, Siregar JP, Cionita T, Prawisudha P, Nugraha FW, Irawan AP, Hadi AE. Mechanical performance analysis of a 3D printing-based transtibial prosthetic socket against the gait cycle using the finite element method. RSC Adv. 2025;15:24150–24166.
17. Palanisamy S, Karuppiah G, Kumar P, Dharmalingam S, Mubarak S, Santulli C, Ayrilmis N, Karumuri S. Effect of process parameters and material selection on the quality of 3D printed products by fused deposition modeling (FDM): A review. Adv Polym Technol. 2024;2024:3480281.
18. Kechagias JD, Ninikas K, Vakouftsi F, Fountas NA, Palanisamy S, Vaxevanidis NM. Optimization of laser beam parameters during processing of ASA 3D-printed plates. Int J Adv Manuf Technol. 2024;130:527–539.

